

1 Meshless method theory

One of the reasons for this development is the fact that mesh-free and mesh-adaptive discretizations are often better suited to cope with geometric changes of the domain of interest, e.g. free surfaces and large deformations, than the classical structured-mesh discretization techniques (FEM-finite element method, FDM-finite difference method, FVM-finite volume method etc). Typically, more than 70 percent of the overall computing time is spent by mesh generators. Since mesh-free discretization techniques are based only on a set of independent points which eliminates the costs of mesh generation. The classical FEM relies on the local approximation properties of polynomials. The method fails when there is high local oscillatory solution or high deformation locally. This can also be understood as that there is a need of high C^k continuity functions (p-refinement) in the FEM literature. Meshless method provides the good solution for this p-refinement problem of FEM with the help of shape functions called Kernel functions without increasing the cost of the solution, and while keeping the reasonable degree of accuracy. Meshless method shape functions has more smoothness which means that one can go to higher order derivative also.

Several meshfree methods have been proposed since the prototype of the meshfree methods (the smoothed particle hydrodynamics (SPH) by Gingold and Monaghan [21] and L. B. Lucy[30]) was born. They are the diffuse element method (DEM) by Nayrole et al. [33], the element free Galerkin method (EFG) by Belytschko et al. [8], the reproducing kernel particle method (RKPM) by Liu et al. [28], the partition of unity finite element method (PUFEM) by Babuska and Melenk [4], the h-p Clouds by Duarte and Oden [14], the moving least-square reproducing kernel method (MLSRK) by Liu et al. [29], the meshless local boundary integral equation method (LBIE) by Zhu et al. [49], the meshless local PetrovGalerkin method (MLPG) by Atluri et al. [2], meshless point collocation methods by Aluru [1], meshless finite point method by Oñate et al.[34] and more.

The development of this method is motivated by the need for new techniques for the solution of problems where the classical FEM approaches fail or are prohibitively expensive; for example, equations with rough coefficients (arising e.g. in the modelling of composites, materials with microstructure, stiffeners, etc) and problems with boundary layers or highly oscillatory solutions fall into that category.

2 SPH

In the traditional SPH method proposed by Gingold and Monaghan [21], the state of the art is represented by a set of particles which possess individual material properties and move according to the governing conservation equations i.e equilibrium equation. Smoothed particle hydrodynamics, as a meshfree, Lagrangian, particle method, has its particular characteristics. It has some special advantages over the traditional grid-based numerical methods, the most significant one among which is the adaptive nature of the SPH method. This adaptability of SPH is achieved at the very early stage of the field variable approximation that is performed at each time step based on a current local set of arbitrarily distributed particles or in other words with the help of kernel function of compact support which make sure that the value at any particle is consistent with the neighbouring particles within the compact support. Because of this adaptive nature of the SPH approximation, the approximation is not affected by the arbitrariness of the particle motion. Therefore, it can naturally handle problems with extremely large deformation. This is, therefore, the most attractive feature of the SPH method. SPH is derived in two step process: first the kernel approximation and the second is particle approximation as mention below. Theoretically exact value of any generic function at any point can be computed by taking the convolution of the function with dirac function.

$$f(x)|_I = \int_{\Omega} f(x)\delta(x - x_I)d\Omega \quad (1)$$

The dirac delta function can be loosely thought of as a function on the real line which is zero everywhere except at the point location x_I , where it is infinite

$$\delta(x - x_I) = \begin{cases} \infty, & x = x_I \\ 0, & x \neq x_I \end{cases} \quad (2)$$

and which is also constrained to satisfy the identity

$$\int_{-\infty}^{\infty} \delta(x) dx = 1 \quad (3)$$

Since the dirac function is hypothetical function, and its difficult to talk about its continuity and differentiability at any point. Therefore there is a need which can substitute well the dirac function. In the same spirit, the first approximation is introduced by using the smoothed function $W_I(x)$, also called Kernel function in place of dirac function.

$$f^h(x)|_I = \int_{\Omega} f(x)W(x - x_I, h)d\Omega \quad (4)$$

where h is called the smoothing length of the kernel function. The kernel function are compact in nature which means that they are non zero positive in small domain while zero elsewhere. The smoothing length governs the shape and the amplitude of the kernel function. When the smoothing length $h \rightarrow 0$ the kernel can be approximated by the Dirac delta function.

$$\lim_{h \rightarrow 0} W(x, h) = \delta(x) \quad (5)$$

The second approximation called particle approximation is employed at this stage to solve the above (eq. 4) numerically, which is being used in computational analysis. This can be achieved by discretization of the continuous domain Ω into the small patches $\Delta\Omega_J$ as

$$f^h(x)|_I = \sum_J f_J W_I(x_J)\Delta\Omega_J \quad (6)$$

In the similar way the approximation of the gradient of the generic function $f(x)$ is derived. For example replacing the function $f(x)$ in (eq. 4) by $\nabla f(x)$ can be represent as

$$\nabla f^h(x)|_I = \int_{\Omega} \nabla f(x)W(x - x_I, h)d\Omega \quad (7)$$

By applying the integration by parts, above equation can be rewritten as

$$\nabla f^h(x)|_I = \int_{\partial\Omega} f(x)W(x - x_I, h)nd\partial\Omega - \int_{\Omega} f(x)\nabla W(x - x_I, h)d\Omega \quad (8)$$

Due to the compact support property of the choosed kernel function, the first term of the right hand side approaches to zero. But this term will not tends to zero when the particle location is on the boundary or near boundary of the domain. Moving from (eq. 1) to (eq. 6) reproducibility is lost. This deficiency has important consequences for the resolution of boundary value problems in terms of accuracy, stability and

convergence of the approximation[42]. This convergence problem will be addressed later in this report. Now further with the help of the second approximation, we can rewrite the equation as,

$$\nabla f^h(x)|_I = - \sum_J f_J \nabla W_I(x_J) \Delta \Omega_J \quad (9)$$

But due to the convergence reason for the non-uniform particle distribution, the equation is modified to the following

$$\nabla f^h(x)|_I = \sum_J [f_I - f_J] \nabla W_I(x_J) \Delta \Omega_J \quad (10)$$

which adds one more property of the suitable kernel function should meet that the derivative of the kernel function is anti-symmetric in the domain at about any point location or mathematically by saying

$$\int_{\Omega} \nabla W_I(x_J) d\Omega = 0 \quad (11)$$

In particular, SPH methods are widely used for fast transient dynamic simulations, such as explosions or impact problems, because of their low computational cost and its ability to handle severe distortions. Other meshless methods, such as EFG or RKPM, can also deal with large distortions and go beyond finite element computations, but with a higher computational cost (due to the use of Gauss quadratures or specific techniques to accurately integrate the weak form). In its original form SPH had several weak points, described in detail in Swegle et al. [43] and Belytschko et al. [6] and Xiao et al. [46], and also Huerta et al. [24] for a review. These problems listed as:

1. Lack of Consistency or completeness [7].
2. Tensile instability [46, 43, 15].
3. Applying essential boundary conditions.
4. Presence of zero-energy modes or the oscillatory modes in the numerical solution[46].

Some of the measures proposed in literature to cure these drawbacks are re-mentioned here in this work later.

2.1 Kernel Functions

Since the kernel is the key element in the SPH methodology, this should be primary concern to any user of SPH. In the paper[20] analyzed the measures of merit for one-dimensional SPH kernel functions. Various kernels with a compact support have been established[20], such as super Gaussian kernels, spline kernels, polynomial kernels and cosine kernels etc. The computational range of these kernels is usually no more than three times the smoothing length. Its concluded there that the key variables in a kernel's worth is its shape and the ration of the particle separation with respect to smoothing length, $\Delta x/h$. Its being approved that bell shaped kernel functions (Gaussian kernel functions) and Q-spline kernels can be regarded as the best kernels [20, 23] in approximation as compared to other kernel functions. Kernel function should try to meet the same properties as the dirac function listed below.

- Positive in its domain
- Integral of the kernel over entire domain is equal to one, $\int_{\Omega} W_i(x)d\Omega = 1$
- Continuous higher derivatives.
- Defined in compact support

Various kernels with a compact support have been established[20], such as super Gaussian kernels, spline kernels , polynomial kernels and cosine kernels etc.

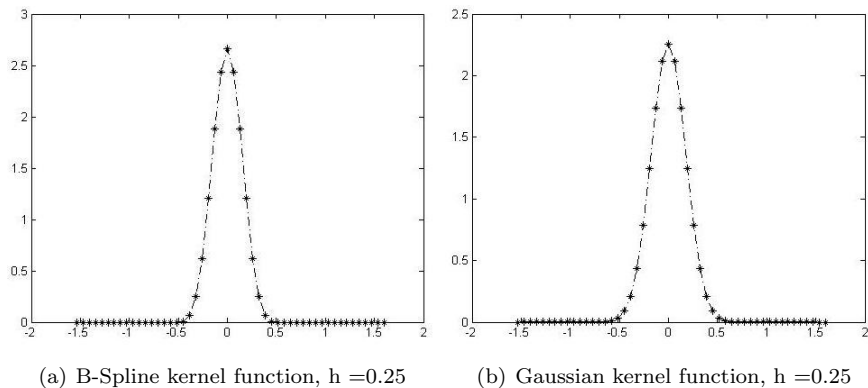


Figure 1: Kernel functions

An example of kernel function is given in Figure 1. where a Gaussian function and B-spline function is depicted. Their expression are given as respectively

Gaussian kernel function in 1-D is given by

$$W(x) = \frac{1}{(\Pi h^2)^{n/2}} \exp\left[-\frac{x^2}{h^2}\right] \quad (12)$$

where x is the distance measured from the center, n is the dimension of the space and h is the smoothing length.

Similarly, B-spline function in 1-D is given by

$$W(r, h) = \begin{cases} \frac{1}{h} \left(\frac{2}{3} - r^2 + \frac{r^3}{3} \right), & 0 < r < 1 \\ \frac{1}{6h} (2 - r)^3, & 1 \leq r < 2 \\ 0, & r \geq 2 \end{cases} \quad (13)$$

where $r = \frac{\|x\|}{h}$, measured from the center and h is the smoothing length

3 Consistency, Completeness and reproducing conditions

In the finite-difference literature the consistency of an approximation is defined by its ability to exactly represent the differential equation in the limit as the number of grid points goes to infinity and the maximum distance between neighbouring grid points goes to zero. Consistency plus stability implies convergence. . As mentioned before moving from (eq. 1) to (eq. 6) reproducibility is lost, and there is great need of correcting the kernel functions of traditional SPH to meet the convergence criterion at the boundary. Two types of correction are proposed in literature. We can employ correction either to the approximating functions, or to the derivatives in order to have the completeness of the approximating functions.

An approximation $f^h(x)$ is complete to order k if any polynomial up to order k can be represented exactly.

$$f^h(x) = \sum_I \Phi_I(x) f_I \quad (14)$$

where $\Phi_I(x)$ are approximating functions and f_I are the nodal values. If the nodal values are given by a polynomial, i.e

$$f_I = a_0 + a_1 x_I + a_2 x_I^2 + \dots + a_k x_I^k \quad (15)$$

then the reproducing conditions (and completeness) of order k are met if

$$f^h(x) = \sum_I \Phi_I(x) f_I = a_0 + a_1 x + a_2 x^2 + \dots + a_k x^k \quad (16)$$

By the above equation we can obtain the following conditions

$$\sum_I \Phi_I = 1 \quad (17)$$

$$\sum_I \Phi_I x_I = x \quad (18)$$

$$\sum_I \Phi_I x_I^2 = x^2 \quad (19)$$

...

$$\sum_I \Phi_I x_I^k = x^k \quad (20)$$

As proposed in the literature that we can employ correction to the derivative also for reproducing the approximating functions completely. Computationally the cost for the corrected derivative is less as compared to the corrected approximating function for reproducing the functions completely. This can be obtained by taking the derivatives of above equations. For example, the linear derivative reproducing conditions for functions in 1D can be written as

$$\sum_I \Phi_{I,x} = 0 \quad (21)$$

$$\sum_I \Phi_{I,x} x_I = 1 \quad (22)$$

For correction of the approximating function, some following approaches are proposed. In the bracket it is mentioned the order of the polynomial that the following correction can able to reproduce exactly.

1. Shepard Correction.[41] (constant functions only)
2. Moving least square approach.[27](desired k^{th} order function)
3. Reproducing kernel particle approach.[27](desired k^{th} order function)
4. Radial basis function.

We can also employ the derivative corrections to reproduce function completely. Several approaches are examined with some mentioned below:

1. Symmetrization given in Monaghan.[32]
2. Johnson and Beissel Correction.[25](linear functions)
3. Randles and Libersky renormalization.[40](constant or linear functions)
4. Krongauz and Belytschko correction.[26](linear functions)

3.1 Correction of approximating function

The first approach to insuring completeness in kernel approximations is to correct the approximation function so that it satisfies the required reproducing conditions. After the correction is made on the approximation, the derivatives of the approximation will satisfy the corresponding derivative reproducing conditions. Expanding the Taylor series for $f(x)$ about x_I , and multiplying both sides by a kernel function, and integrating over the domain Ω yields,

$$\begin{aligned} \int_{\Omega} f(x)W_I(x)dx &= f(x_I) \int_{\Omega} W_I(x)dx + f_x(x_I) \int_{\Omega} (x - x_I)W_I(x)dx \\ &+ f_{xx}(x_I) \int_{\Omega} (x - x_I)^2 W_I(x)dx + \dots \end{aligned} \quad (23)$$

where $f_x = \frac{df}{dx}$, $f_{xx} = \frac{d^2f}{dx^2}$, and $W_I(x) = W(x - x_I, h)$. By the symmetry property of the kernel function, coefficients of the first derivative terms on the right side of the above equation tends to zero, except near the boundary, which means the following at the boundary,

$$\begin{aligned}\int_{\Omega} (x - x_I) W_I(x) dx &\cong \int_{\Omega} \Theta(h) W_I(x) dx \\ \int_{\Omega} (x - x_I)^2 W_I(x) dx &\cong \int_{\Omega} \Theta(h^2) W_I(x) dx\end{aligned}\tag{24}$$

The above equations can be corrected so that it tends to zero by making correction to the kernel function or in other words make the inherent property of the choosed kernel function.

Therefore the (eq. 23) can be rewritten as by dropping the truncation error terms (eq. 24),

$$f(x)_I \cong \frac{\int_{\Omega} f(x) W_I(x) dx}{\int_{\Omega} W_I dx}\tag{25}$$

For those points x_I far away from a boundary, the integral of $W_I(x)$ is equal to 1. Hence, (eq. 25) reduces to the conventional kernel estimate, (eq. 6). The truncation error is on the order of $(x - x_I)^2$ or h^2 in the interior of the domain whereas on the order of $(x - x_I)$ or h for x_I near or on the boundary because the integral of the product $(x - x_I) W_I(x)$ is no longer equal to zero. The difference between (eq. 4) and (eq. 25) is clear. Ignoring the correction term (denominator term), i.e. the integral of $W_I(x)$ in (eq. 25), is the essential factor for causing the boundary deficiency in the conventional kernel estimate. In the similar way, we can approach to the correction of the derivative of the approximating function by replacing $W_I(x)$ with $W_{I,x} = \frac{\partial W_I(x)}{\partial x}$. The following expression is generated by manipulation of the (eq. 23)

$$f(x)_I \cong \frac{\int_{\Omega} [f(x) - f(x_I) W_{I,x}] dx}{\int_{\Omega} (x - x_I) W_{I,x} dx}\tag{26}$$

Since by the property of the kernel function that the first derivative of the kernel function is antisymmetric, denominator of the (eq. 26) will not become zero. The truncation error is of order of h^2 in the interior domain and of order h near the boundary. The following section mention the two general approach for correcting the approximating function to the desired k^{th} order reproducibility.

3.1.1 Moving Least Square approach

Moving least square is the approach to achieve the corrected kernel function. Moving least square is the similar term that is used in Statistics to fit the curve among the scattered data points. Assume the interpolating function $f^h(x)$ in the form

$$f^h(x) = f^h(x, a_0, a_1, \dots, a_I)\tag{27}$$

where the parameters a_0, \dots, a_I are determined by minimizing the error. (for each fixed x ; therefore, strictly speaking, the coefficients depend on x). The local character of the moving least-squares (MLS) approximation, i.e. the moving part, arises from the dependence of parameters a_I on x which further depends on the kernel window.

$$L = \sum_I [f_I - f^h(x_I, a_0, \dots, a_I)]^2 W_I(x)\tag{28}$$

This method is called moving least squares method. By minimization of the above equation, the parameters are determined, and the global approximation $f^h(x)$ takes the form

$$f^h(x) = \sum_I \Phi_I(x) f_I\tag{29}$$

Construction: In the moving least square approximation, we let

$$f^h(x) = \sum_I p_I(x) a_I(x)\tag{30}$$

Here I is the number of terms in the basis, $p_I(x)$ are monomial basis functions, and $a_I(x)$ are their coefficients, which as indicated, are functions of the spatial coordinates x . The commonly used bases for the linear and quadratic basis in 1-D are

$$\mathbf{p}^T = (1, x) \quad \mathbf{p}^T = (1, x, x^2) \text{ in } 1D, \quad (31)$$

The coefficients $a_I(x)$ are obtained by minimizing the difference between the local approximation value and the function value at any given point. This yields the quadratic form

$$\begin{aligned} J &= \sum_J W(x - x_J) (f^h(x, x_J) - f(x_J))^2 \\ &= \sum_J W(x - x_J) \left[\sum_I p_I(x_J) a_I(x) - f_J \right]^2 \end{aligned} \quad (32)$$

where $W(x - x_J)$ is a weighting function with compact support; the same weight functions as in SPH are used. Note that the term corresponding to $f^h(x)$ in (eq. 32) consists of the monomials at x_J and the coefficient at x . Above equation can be rewritten in the form as

$$J = ((\mathbf{P}\mathbf{a} - \mathbf{u})^T \mathbf{W}(\mathbf{x}) (\mathbf{P}\mathbf{a} - \mathbf{u})) \quad (33)$$

where $\mathbf{f}^T = (\mathbf{f}_1, \mathbf{f}_2 \dots \mathbf{f}_n) = \mathbf{u}^T = (\mathbf{u}_1, \mathbf{u}_2 \dots \mathbf{u}_n)$. The change of symbol is used here just for brevity.

$$\mathbf{P} = \begin{bmatrix} p_1(x_1) & p_2(x_1) & \dots & p_m(x_1) \\ p_1(x_2) & p_2(x_2) & \dots & p_m(x_2) \\ \vdots & \vdots & \ddots & \vdots \\ p_1(x_n) & p_2(x_n) & \dots & p_m(x_n) \end{bmatrix} \quad (34)$$

and

$$\mathbf{W}(\mathbf{x}) = \begin{bmatrix} W(x - x_1) & 0 & \dots & 0 \\ 0 & W(x - x_2) & \dots & 0 \\ \vdots & \vdots & \ddots & \vdots \\ 0 & 0 & \dots & W(x - x_n) \end{bmatrix} \quad (35)$$

To find the coefficients $\mathbf{a}(\mathbf{x})$, we obtain the extremum of J by

$$\frac{\partial J}{\partial \mathbf{a}} = \mathbf{A}(\mathbf{x})\mathbf{a}(\mathbf{x}) - \mathbf{B}(\mathbf{x})\mathbf{u} = \mathbf{0}, \quad (36)$$

where \mathbf{B} is called the moment matrix and is given by

$$\mathbf{A} = \mathbf{P}^T \mathbf{W}(\mathbf{x}) \mathbf{P} \quad (37)$$

$$\mathbf{B} = \mathbf{P}^T \mathbf{W}(\mathbf{x}) \quad (38)$$

The approximation $f^h(x)$ can then be expressed as

$$f^h(x) = \sum_J \Phi_J^k(x) f_J, \quad (39)$$

where the shape functions are given by

$$\Phi^k = [\Phi_1^k(x) \dots \Phi_n^k(x)] = \mathbf{p}^T \mathbf{A}^{-1}(\mathbf{x}) \mathbf{B}(\mathbf{x}), \quad (40)$$

where the superscript k is the order of the polynomial basis. The above $\Phi_j^k(x)$ are the corrected kernel function of the consistency or reproducibility of order k . The spatial derivatives of the shape functions are obtained by

$$\begin{aligned} \Phi_{I,x} &= (\mathbf{p}^T \mathbf{A}^{-1} \mathbf{B}_I)_{,x} \\ &= \mathbf{p}_{,x}^T \mathbf{A}^{-1} \mathbf{B}_I + \mathbf{p}^T (\mathbf{A}^{-1})_{,x} \mathbf{B}_I + \mathbf{p}^T \mathbf{A}^{-1} \mathbf{B}_{I,x} \end{aligned} \quad (41)$$

where

$$\mathbf{B}_{I,x} = \frac{dw}{dx} (x - x_I) \mathbf{p}(\mathbf{x}_I) \quad (42)$$

and $\mathbf{A}^{-1}_{,x}$ is computed by

$$\mathbf{A}^{-1}_{,x} = -\mathbf{A}^{-1} \mathbf{A}_{,x} \mathbf{A}^{-1} \quad (43)$$

where

$$\begin{aligned} \mathbf{A}_{,x} &= \sum_{I=1}^n w(x - x_I) \mathbf{p}(x_I) \mathbf{p}^T(x_I) \\ &= \frac{dw}{dx} (x - x_1) \begin{bmatrix} 1 & x_1 \\ x_1 & x_1^2 \end{bmatrix} + \frac{dw}{dx} (x - x_2) \begin{bmatrix} 1 & x_2 \\ x_2 & x_2^2 \end{bmatrix} \\ &\quad + \dots \frac{dw}{dx} (x - x_n) \begin{bmatrix} 1 & x_n \\ x_n & x_n^2 \end{bmatrix} \end{aligned} \quad (44)$$

Similarly, the second derivative expression can be derived by chain rule

$$\begin{aligned} (\Phi_{I,x})_{,x} &= (\mathbf{p}_{,x}^T)_{,x} \mathbf{A}^{-1} \mathbf{B}_I + \mathbf{p}_{,x}^T (\mathbf{A}^{-1})_{,x} \mathbf{B}_I + \mathbf{p}_{,x}^T \mathbf{A}^{-1} \mathbf{B}_{I,x} \\ &\quad \mathbf{p}_{,x}^T (\mathbf{A}^{-1})_{,x} \mathbf{B}_I + \mathbf{p}^T ((\mathbf{A}^{-1})_{,x})_{,x} \mathbf{B}_I + \mathbf{p}^T (\mathbf{A}^{-1})_{,x} \mathbf{B}_{I,x} \\ &\quad \mathbf{p}_{,x}^T \mathbf{A}^{-1} \mathbf{B}_{I,x} + \mathbf{p}^T (\mathbf{A}^{-1})_{,x} \mathbf{B}_{I,x} + \mathbf{p}^T \mathbf{A}^{-1} (\mathbf{B}_{I,x})_{,x} \end{aligned} \quad (45)$$

where

$$\begin{aligned} (\mathbf{A}^{-1}_{,x})_{,x} &= -(\mathbf{A}^{-1} \mathbf{A}_{,x} \mathbf{A}^{-1})_{,x} \\ &= -(\mathbf{A}^{-1})_{,x} \mathbf{A}_{,x} \mathbf{A}^{-1} - \mathbf{A}^{-1} (\mathbf{A}_{,x})_{,x} \mathbf{A}^{-1} - \mathbf{A}^{-1} \mathbf{A}_{,x} (\mathbf{A}^{-1})_{,x} \end{aligned} \quad (46)$$

3.1.2 Reproducing kernel particle approach

Reproduce Kernel approach was developed by Liu et al. [28] in order to reproduce the approximating function correctly. By introducing the correction function, the kernel function in kernel estimate is modified to satisfy the consistency condition in any arbitrary domain of problems and, as a result, the shape function of the method and its derivatives are derived.

It involves the correction to the kernel function as

$$K_I(x) = C_I(x)W_I(x) \quad (47)$$

In the above expression $W_I(x)$ is the SPH kernel function, while $C_I(x)$ function is the correction function. In order to obtain the desired reproducing properties $C_I(x)$ assumes the following relationship

$$C_I(x) = b_{0I} + b_{1I}(x - x_I) + \dots \quad (48)$$

As mentioned in the section 3.1, the truncation error can be pushed to higher order terms if the choosed kernel function posses the following property.

$$p_0 = \int_{\Omega} K_I(X)dx = 1 \quad (49)$$

$$p_1 = \int_{\Omega} (x - x_I)K_I(X)dx = 0 \quad (50)$$

$$p_2 = \int_{\Omega} (x - x_I)^2 K_I(X)dx = 0 \quad (51)$$

The above equation can be rewritten again with the help of the (eq. 48) as following considering the consistency only upto first order term.

$$p_0 = \int_{\Omega} (b_{0I} + b_{1I}(x - x_I))W_I(X)dx = 1 \quad (52)$$

$$p_1 = \int_{\Omega} (x - x_I)(b_{0I} + b_{1I}(x - x_I))W_I(X)dx = 0 \quad (53)$$

Further defining the following in the discretized form,

$$m_0 = \sum_J W_I(x_J)dx_J \quad (54)$$

$$m_1 = \sum_J (x_J - x_I)W_I(x_J)dx_J \quad (55)$$

$$m_2 = \sum_J (x_J - x_I)^2 W_I(x_J)dx_J \quad (56)$$

Then, the following system of equation is obtained from (eq. 52-53)

$$\begin{aligned} b_{0I}m_0 + b_{1I}m_1 &= 1 \\ b_{0I}m_1 + b_{1I}m_2 &= 0 \end{aligned} \tag{57}$$

Solving for b_{0I}, b_{1I} from the above equations and back substitution to the (eq. 47) will give the required corrected kernel function of first order consistency.

The basic idea of meshless methods[42] is to use shape functions which are used in fitting of points. More precisely, given a distribution of nodes x_I , the fitting algorithm (moving least square or reproducing kernel approximant) is invoked to produce the shape functions, Φ_I which are then used in the discretization of the continuum in either method Galerkin or Collocation method. These shape functions are used in a Galerkin or collocation discretization process to set up a linear system of equations. All these data fitting approaches do not depend (at least to a great extent) upon a mesh or any fixed relation between grid points (particles). However, the realization and implementation of such a method is not so simple in general: there are often problems with stability and consistency conditions.

4 Discretization

The discretization scheme employed in the meshfree numerical simulation is presented in this section. In the work reported so far, the following method of discretization schemes are well renowned, namely

1. Collocation methods [1]
2. Galerkin methods [8, 37, 17]
3. Mixed Galerkin-Collocation methods.[11]

Each methods has some advantages and disadvantages in itself. Galerkin-based meshless method are computational intensive, whereas collocation-based meshless methods suffer from instability (Tensile instability and rank deficiency). Lets consider the example of imposing collocation method and Galerkin methods on the conservation of linear momentum equation in Lagrangian formulation.

$$\rho_0 \ddot{u} = \nabla_X \cdot P + \rho_0 b \tag{58}$$

where ρ_0 initial densities, \ddot{u} material time derivatives of displacement vector, ∇_X is the gradient or divergence operator expressed in material derivatives, P is the nominal stress tensor and b is the body force. The boundary conditions are following

$$u(X, t) = \bar{u}(X, t) \quad \Gamma_0^u \tag{59}$$

$$n^0 \cdot \mathbf{P}(X, t) = \bar{t}(X, t) \quad \Gamma_0^t \tag{60}$$

where \bar{u} and \bar{t} are the prescribed displacement and traction values on the boundary, respectively, n^0 is the outward normal to the domain and $\Gamma_0^u \cup \Gamma_0^t = \Gamma_0$, $\Gamma_0^u \cap \Gamma_0^t = \emptyset$

4.1 Collocation Based Method

In collocation methods the discrete equations are obtained by enforcing the equilibrium equation on the set of nodes. Now by enforcing the kernel approximation mentioned in (eq. 9) to the governing (eq. 58) at particle I in domain is represented as

$$\rho_0 \ddot{u}_I = \sum_J \nabla_X W_{IJ} \cdot P_J \Delta \Omega_J + \rho_0 b \quad (61)$$

The above equation are simply linear algebraic equation system and could be solved by any of the standard methods. It should be noted that some more algebraic linear system equations comes from boundary conditions. Hence in this method there are more number of equations than actually the number of unknowns. Nodal integration is used to solve the above equation which encompasses instability due to rank deficiency and tensile instability. Stress point integration could be used to remove rank deficiency, but tensile instability could not be eliminated [46].

As an attempt to avoid the weak form Galerkin method, a least-square formulation was suggested [38] but proved to be adequate only for lower-order schemes such as those for first-order partial differential equations. As an alternative approach, Oñate et al. [35] developed a point collocation scheme for fluid flow problem on the basis of weighted least-squares procedure, which they called the finite point method. The finite point method includes additional terms in the strong form to stabilize the convective term. Oñate et al. [36] also applied this method to elasticity problems. Aluru [1] and Zhang et al. [48] presented point collocation methods based on the reproducing kernel approximation and radial basis functions, respectively. Zhang et al. [47] proposed a least-squares collocation meshfree method which uses auxiliary points to improve the solution accuracy.

4.2 Galerkin Based Method

Galerkin Based formulation is the standard method that is used in FEM formulation also. One of the essential ingredient of the Galerkin formulation is the integration by parts and the application of the divergence theorem. Using the same ideology (eq. 58) can be framed in galerkin method as

$$\int_{\Omega_0} \rho_0 \delta u \cdot \ddot{u} d\Omega = \int_{\Omega_0} \rho_0 \delta u \cdot b d\Omega - \int_{\Omega_0} (\nabla_X \delta u)^T : P d\Omega + \int_{\Gamma_0} \delta u \cdot \bar{t} d\Gamma \quad (62)$$

where δu is the test function from its right candidate Hilbert space set which is here in this case the subset of corrected Kernel functions. Now imposing corrected SPH approximation to the above equation will give

$$m_I \ddot{u}_I = f_I^{ext} - f_I^{int}, \quad (63)$$

$$f_I^{ext} = \int_{\Omega_0} \rho_0 W_I b d\Omega + \int_{\Gamma_0} W_I \bar{t} d\Gamma \quad (64)$$

$$f_I^{int} = \int_{\Omega_0} (\nabla_X W_I)^T \cdot P d\Omega \quad (65)$$

Galerkin methods require some type of cell structure for integration over the problem domain. This procedure assumes exact integration and thus inaccuracy in the integration is directly related to the solution accuracy. Although Galerkin-based meshfree methods have advantageous features, difficulties of imposing essential boundary conditions and undeniable usage of background cell for Galerkin formulation erode merits of meshfree methods. Nodal integration, cell or octree quadrature, and background finite element mesh quadrature have been used. The first of these is the fastest, but appears to suffer from instability [5] and several stabilization schemes have been developed. The second and third have the disadvantage that the resulting method is not truly meshless. In Galerkin based meshless method (GBMM), derivatives in domain integrals are lowered by using the divergence theorem to establish the weak form. The inaccuracy in integration will result in significant error in the solution. However, the shape functions in meshless method are very complex. Delicate background cells and a large number of quadrature points must generally be employed to integrate the weak form as accurate as possible. As a consequence, the GBMM is much more expensive than FEM.

4.3 Integration Schemes

The computational efficiency of mesh free Galerkin methods hinges critically on the choice of domain quadrature, and the issue is more computationally critical in fast dynamics and iterative equilibrium. The shape functions in meshfree methods are rational functions of the spatial coordinates and their local supports may not align with the integration domains. This misalignment is the more significant source of error and affects the accuracy and convergence of meshfree methods[13]. The article [13]also proposes the technique bounding box to impose the alignment of the kernel supports with the integration domain. Note that in case of FEMs supports and integration domains always coincide. Accurate integration of the weak form requires for more quadrature points than in finite element methods. Hence the computational demand of mesh free methods to employ quadrature rules is quiet high as compared to FEMs. The major issues with discretization of the continuum via Galerkin is the evaluation of the integrals of the eq. 61 and eq. 64-65. There has some proposed approaches mentioned here.

1. Nodal integration , where the integral is evaluated by

$$\int_{\Omega} f(x)d\Omega = \sum_{I=1}^n f(x_I)\Delta\Omega_I \quad (66)$$

This is the nodal integration scheme[17] posses the same stability properties as of SPH, which is truly meshless method. The nodal integration is used in collocation methods for evaluating the integrals term. Though this integration is very fast and most suitable e.g for fast transient dynamics problems but this approach gives unstable results for integrating higher order differential equation i.e second order or higher. This need the further careful study for this instabilities which is also not much touched part in the literature. Quadrature schemes that employ only the nodes (also called the particles) as quadrature points, are only moderately slower than the FEM; however, they tend to exhibit instabilities[6, 39]. This problem has been addressed by Beissel and Belytschko [5] and Chen et al. [10], where least-squares stabilization for nodal integration is proposed. Nevertheless, many remarkable solutions have been obtained by standard SPH.

2. Cell or octree quadrature where a regular array of domains in the background is used for quadrature. This approach cost more than the finite element method computationally because the mesh free approximants are non-polynomial in character and required more integration points.

3. Stress point integration approach.

Actually its not the new approach but a remedy proposed by Dyka et al. [15, 16] to stabilize the standard SPH method or nodal integration method. The convergence and stability properties of stress-point integration are between full integration and nodal integration; the later can be considered unstable. The numerical studies that for uniform arrangements of particles, stress point integration achieves good convergence rates. However, for non-uniform arrangements of particles fail to converge. Least square stabilization is used with stress point integration to get more stabilization and convergence for non-uniform arrangement of particles[19]. Randles et al. [40] extended stress point integration to higher dimensions to stabilize the normalized form of SPH. Stress point integration eliminates instabilities due to rank deficiency but not those due to the tensile instability, see Belytschko et al. [46]. Stress point integration is used when nodal integration is employed either in collocation method or Galerkin method for removing spurious modes or oscillatory modes (rank deficiency instability). This is used only in evaluating the internal force term. eq. 65 can be represented as the following using extra integration points called stress points by

$$f_I^{int} = \sum_{J1} V_{J1}^0 \nabla_X W_I(X_{J1}) \cdot P_{J1} + \sum_{J2} V_{J2}^0 \nabla_X W_I(X_{J2}) \cdot P_{J2} \quad (67)$$

where J1 and J2 are subsets of master nodes and stress points respectively.

In the second and third cases Gauss quadratures or specific techniques are employed to accurately integrate[42] the weak form. In the EFG method, the integrals of eq. 64-65 are usually evaluated over background cells based on an octree structure. Full quadrature in the cells is computationally expensive for nonlinear and or dynamic problems. SPH collocation is equivalent to EFG method when nodal integration strategy is employed, so it will exhibit the same instabilities.

5 Boundary Conditions

Imposing essential boundary conditions is a key issue in mesh-free methods. The shape functions in meshless methods are not strict interpolants, i.e they do not satisfy the Kronecker delta condition

$$N_A(x_B) \neq \delta_{AB} \neq \begin{cases} 1 & \text{if } A = B \\ 0 & \text{otherwise} \end{cases} \quad (68)$$

where $N_A(x_B)$ is the shape function of node A evaluated at node B, and δ_{AB} is the Kronecker delta. In other words the shape function associated to a particle does not vanish at other particles, which is not the case with Finite element method. A consequence of this is that the approximated value on the boundary depends on interior nodes as well as boundary nodes. For example this prevents the treatment like finite element method for Dirichlet boundary conditions, where boundary nodes are simply omitted from the solution procedure. Some of the proposed technique for implementing the essential boundary conditions in mesh free methods are mentioned. These techniques can be classified in following groups:

1. methods based on a modification of the weak form, such as Lagrange multiplier method[8], the penalty method [49]and Nitsche's method[22, 3]
2. methods in which coupling is achieved between the meshfree shape functions and the finite element shape function near the boundary, which allows directly to impose prescribed values. Coupling between FE and SPH [31]or between FE and EFG or RKPM [9, 24]is used to deal with boundary conditions

problem. On the other hand, bridge scale method proposed in [44] is a general technique to mix a mesh-free approximation with any other interpolation space, in particular with finite elements near the essential boundary.

The most excellent review for imposing the boundary conditions in mesh free method could be found in [18].

6 Stability and Convergence of Meshfree methods

The stability of the particle (meshfree) method is essential to their robustness. Three kinds of instabilities mainly results from the discretization of the continua are mentioned in literature so far namely:

1. a high frequency instability which results from the rank deficiency of the discrete divergence operator and makes the equilibrium equations singular; this occurs regardless of the value of the stress.
2. a tensile instability which results from the interaction of the second derivative of kernel and the tensile stress, it occurs even in one-dimensional plane response or also defined premature fragmentation of the SPH grid in tension.
3. Material instability which is also found in continua.

The tensile instability was first identified by Swegle et al. [43] by a Neumann analysis of the one-dimensional equation. This behavior is synonym to the under-integration of the Galerkin form which leads to spurious singular modes(also called node to node oscillation in some of the reviews) in the solution space. This is analogous to hourglass control for reduced integration in finite element techniques. Stability is a primary concern for any nodal integration method since large oscillations in the solution can often occur unless some measures are taken to mitigate them. In lieu of stabilization, stress points are often introduced near the nodes to avoid these oscillations.

Stress-point integration was first proposed by Dyka and Ingel [15] and Dyka et al. [16] for tension instabilities in SPH. In fact, stress points do not suppress tension instabilities, which are due to a rather anomalous description of the motion in SPH, see [6]. Instead, in many cases they restore the positive definiteness of the linear equations, i.e. they correct rank deficiency. Stress-point integration for multi-dimensions was proposed by Randles et al.[40], who use only the stress points for quadrature. The convergence and stability properties of stress-point integration are between full integration and nodal integration; the latter can be considered unstable.

Some review is mentioned in the article[6] regarding the stability analysis of meshfree methods with Eulerian and Lagrangian kernels formulation. It was concluded in the article that instability due to rank deficiency occurs for both Lagrangian and Eulerian kernels with nodal integration or collocation. This instability can be eliminated by stress points. However, it is found stress points cannot completely stabilize Eulerian kernels. It will be shown that the tensile instability is to a large extent the idiosyncrasy of what we call Eulerian kernels. In an Eulerian kernel, the stability depends on the stress and the second derivative of the kernel. This generates the tensile instability. When the kernel is function of the material(Lagrangian) co-ordinates, a so- called Lagrangian kernel, the tensile instability does not occur. It was also concluded that the best approach to stable particle discretizations is to use Lagrangian kernels with stress points. However the convergence and stability depends on the distribution of the particles on the domain, which give very poor convergence for non-uniform particle distribution. It was concluded that stability can be achieved in

irregular particle distribution by least-square stabilization. The following methods proposed so far in the realm for the stabilization of meshfree methods.

1. Swegle et al. [45] have proposed a conservative smoothing scheme to eliminate the tensile instability.
2. The short wave length modes can be suppressed with Least square stabilization [5, 10] for nodal integration stability which contains the square of the residual of the momentum equation in the weak form.
3. Stabilization by stress point technique which suppresses high frequency instability.

7 Numerical Simulation

Some of the numerical simulation for the solution of the differential equation is presented in this section. It should be noted that Gaussian kernel, W_I is used with smoothing length ($h = 0.225$) in all the examples. The following example illustrates the significance of the uncorrected and corrected standard SPH kernel function in approximating the function. The following function is approximated by the standard SPH method.

$$f(x) = \sin x \quad 0 \leq x \leq \Pi \quad (69)$$

The equations that are used in approximating the above function and its derivative are as.

$$f^h(x)|_I = \sum_J f_J W_I(x_J) \Delta\Omega_J \quad (70)$$

$$\nabla f^h(x)|_I = \sum_J [f_I - f_J] \nabla W_I(x_J) \Delta\Omega_J \quad (71)$$

Figure 2.a-2.b clearly mention the inaccuracy in reproducing the function and its first derivative near the boundaries. After correcting the kernel function by Moving least square approach mentioned in section 3.1.1, Figure 2.c-2.d shows excellent correlation between the exact and approximated function.

7.1 Spatial differential equation

Consider the following one-dimensional second order differential equation on the domain $0 \leq x < 1$

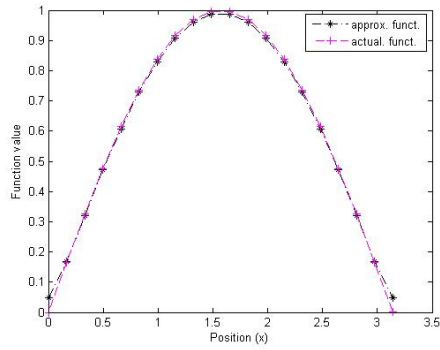
$$\frac{d^2 u}{dx^2} + x = 0 \quad (72)$$

with the following boundary conditions

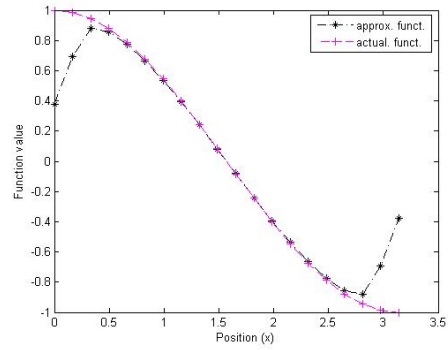
$$\begin{aligned} u(0) &= 0 \\ \frac{du}{dx} \Big|_{x=1} &= 0 \end{aligned} \quad (73)$$

The exact solution to the above problem is given by

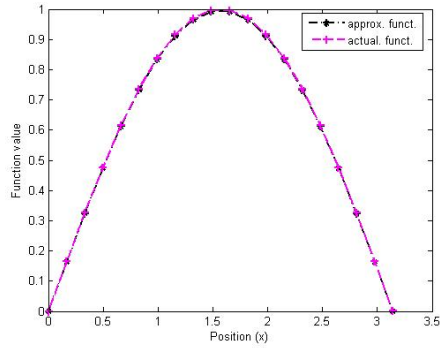
$$u(x) = \left(\frac{x}{2} - \frac{x^3}{6} \right) \quad (74)$$



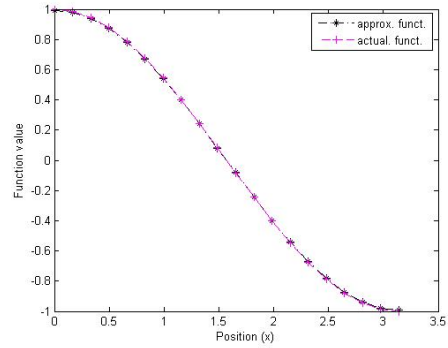
(a) Function approximation



(b) First derivative approximation



(c) Function approximation with corrected kernel

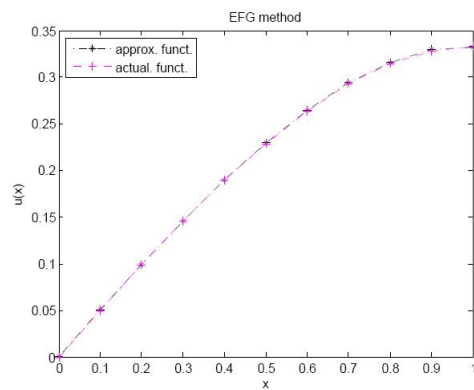


(d) First derivative approximation with corrected kernel

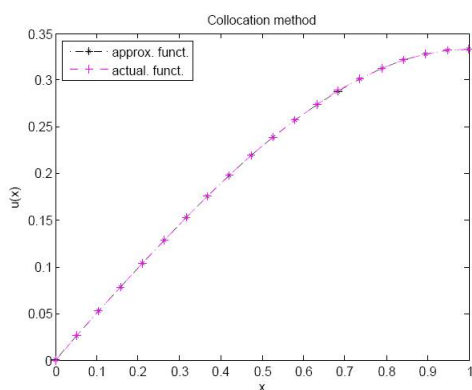
Figure 2: Kernel functions

The above differential equation (eq. 72) is solved by Element free Galerkin method [12]. Weak form is computed under the Galerkin method as specified in section 4.2. Further moving least square approximant is used for the approximated solution. Figure 3a shows the good correlation between the approximated and exact solution.

The differential equation (eq. 72) could also be solved by collocation method. The second order derivative of the shape function is mentioned in (eq. 45). Figure 3b shows the good correlation between the approximated and exact solution by collocation method.



(a) EFG method.



(b) Collocation method.

Figure 3: differential equation solution.

Next example, consider the following one-dimensional first order differential equation on the domain $0 \leq x < \Pi$

$$\frac{du}{dx} = x \quad (75)$$

with the following boundary conditions

$$u(0) = 0 \quad (76)$$

The exact solution to the above problem is given by

$$u(x) = \frac{x^2}{2} \quad (77)$$

The above differential equation (eq. 75) is solved by Collocation based method as mentioned in section 4.1. Further moving least square approximant is used for the approximated solution. Figure 4 shows the good correlation between the approximated and exact solution.

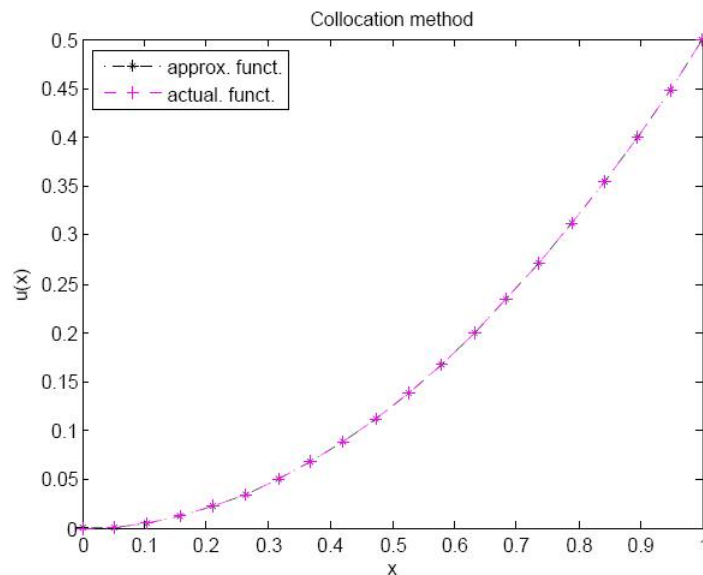


Figure 4: Differential equation solution

7.2 Temporal differential equation

Next example, consider the following one-dimensional wave equation on string with domain $0 \leq x < L$

$$\frac{d^2u}{dt^2} = c^2 \frac{d^2u}{dx^2} \quad (78)$$

where L is the length of the string, c, is wave propagation speed on the string. The following are the boundary conditions

$$\begin{aligned} u(0, t) = u(L, t) &= 0 \\ \frac{du(x, 0)}{dt} &= f(x) \end{aligned} \quad (79)$$

The spatial discretization of the wave equation is achieved with help of collocation methodologies where the second derivative of the shape function is obtained from (eq. 45). Iterative time step is done with the

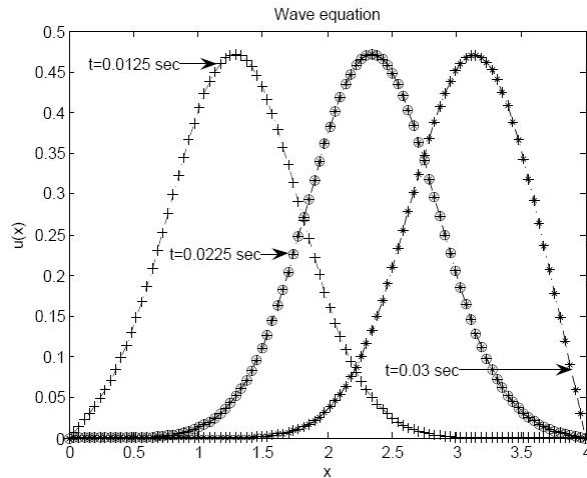
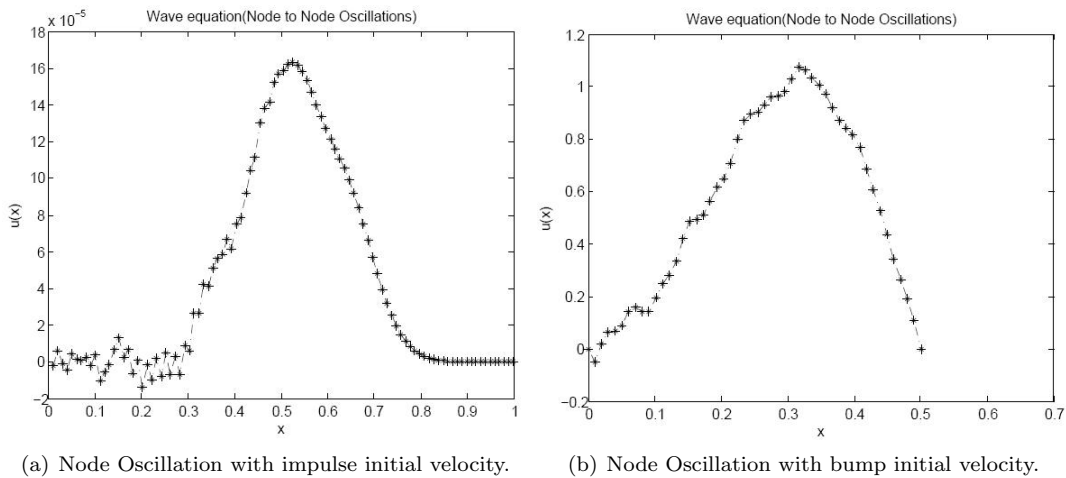


Figure 5: Wave equation solution

help of Leap-frog iterative scheme. Figure 5 shows the propagation wave at three different time shots, with the following parameters $L = 4m, c = 5053m/s, timestep = 0.00025sec$

Instability due to node to node oscillation is depicted in Figure 6 below at some time shots of propagation wave. The following parameters is chosen for showing this instability: Figure 6a $L = 1m, c = 5053m/s, timestep = 0.00000025sec$ with initial velocity = $5m/sec$ to all the particles from $x = 0$ to $x = \frac{L}{4}$. Figure 6b $L = 0.5m, c = 9053m/s, timestep = 0.00000025sec$ with initial velocity a bump function $f(x) = -40xe^{-x^2}$. The solution is clearly no longer smooth which as shown in Figure 5, and clearly shows the numerical integration instability.



(a) Node Oscillation with impulse initial velocity.

(b) Node Oscillation with bump initial velocity.

Figure 6: Wave equation solution.

References

- [1] N. Aluru, *A point collocation method based on reproducing kernel approximation.*, Int. Journl. Numer. Methds. Eng. **47** (2000), no. 6, 1083–1121.
- [2] S. N. Atluri and S. Shen, *The meshless local petrov-galerkin (mlpg) method: a simple and less-costly alternative to the finite element and boundary element methods.*, Computer Model. Eng. and Sci., **3** (2002), no. 1, 11–52.
- [3] I. Babuska, I. Banerjee, and J. E. Osborn, *Meshless and generalized finite element methods: A survey of some major results.*, In Meshfree Methods for Partial Differential Equations, vol. 26, Springer Verlag, Berlin, 2002.
- [4] I. Babuska and J. M. Melenk, *The partition of unity method.*, Int. Journl. Numer. Methds. Eng. **40** (1997), 727–758.
- [5] S. Beissel and T. Belytschko, *Nodal integration of the element-free galerkin method*, vol. 139, pp. 49–74, 1996.
- [6] T. Belytschko, Y. Guo, W. K. Liu, and S. P. Xiao, *A unified stability analysis of meshless particle methods*, Int. Journl. Numer. Methds. Eng. **48** (2000), 1359–1400.
- [7] T. Belytschko, Y. Krongauz, J. Dolbow, and C. Gerlach, *On the completeness of meshfree particle methods*, Int. Journl. Numer. Methds. Eng. **43** (1998), 785–819.
- [8] T. Belytschko, Y. Y. Lu, and L. Gu, *Element-free galerkin methods.*, Int. Journl. Numer. Methds. Eng. **37** (1994), 229–256.
- [9] T. Belytschko, D. Organ, and Y. Krongauz, *A coupled finite element-element free galerkin method.*, Comput. Mech. **17** (1995), no. 3, 186–195.
- [10] J. S. Chen, C. T. Wu, and Y. You, *A stabilized conforming nodal integration for galerkin mesh-free methods.*, Int. Journl. Numer. Methds. Eng. **50** (2001), 435–466.
- [11] G. A. Dilts, *Moving-least squares-particle hydrodynamics-i. consistency and stability*, Int. Journl. Numer. Methds. Eng. **44** (1999), 1115–1155.
- [12] J. Dolbow and T. Belytschko, *An introduction to programming the meshless element free galerkin method.*, Archives Comput. Methd. Eng. **5** (1998), no. 3, 207–241.
- [13] _____, *Numerical integration of the galerkin weak form in meshfree methods.*, Comput. Mech. **23** (1999), 219–230.
- [14] C. A. Duarte and J. T. Oden, *h-p clouds - an h-p meshless method.*, Numer. methods. Partial Differ. Equations, **12** (1996), no. 6, 673–705.
- [15] C. T. Dyka and R. P. Ingel, *An approach for tension instability in smoothed particle hydrodynamics(sph)*, Comp. and Struct. **57** (1995), 573–580.
- [16] C. T. Dyka, P. W. Randles, and R. P. Ingel, *Stress points for tension instability in sph.*, Int. Journl. Numer. Methds. Eng. **40** (1997), 2325–2341.
- [17] L. C. Felgueroso, I. Colominasand G. Mosqueira, F. Navarrina, and M. Casteleiro, *On the galerkin formulation of the smoothed particle hydrodynamics method.*, Int. Journl. Numer. Methds. Eng. **60** (2004), 1475–1512.
- [18] Sonia Fernandez-Mendez and Antonio Huerta, *Imposing essential boundary conditions in mesh-free methods.*, Computer Methds. Appl. Mech. Eng. **193** (2004), 1257–1275.
- [19] T. P. Fries and T. Belytschko, *Convergence and stabilization of stress-point integration in mesh-free and particle methods.*, Int. Journl. Numer. Methds. Eng. **74** (2008), 1067–1087.

- [20] D. A. Fulk and D. W. Quinn, *An analysis of 1-d smoothed particle hydrodynamics.*, Journl. Comput. Physics **126** (1996), 165–180.
- [21] R. A. Gingold and J. J. Monaghan, *Smoothed particle hydrodynamics: theory and application to non-spherical stars.*, Mon. Not. Royal. Astr. Soc. **181** (1977), 375–389.
- [22] M. Griebel and M. A. Schweitzer, *A particle-partition of unity method. part v: Boundary conditions*, Geometric Analysis and Nonlinear Partial Differential Equations, Springer-Verlag, Berlin, 2002.
- [23] J. Hongbin and D. Xin, *On criterions for smoothed particle hydrodynamics kernels in stable field.*, Journl. Comput. Physics **202** (2005), 699–709.
- [24] A. Huerta, T. Belytschko, S. Fernandez-Mendez, and T. Rabczuk, *Meshfree methods*, In Encyclopedia of Computational Mechanics, vol. 1, ch. 10, pp. 279–309, John Wiley and Sons, 2004.
- [25] G. R. Johnson and S. R. Beissel, *Normalized smoothing functions for sph impact calculations*, Int. Journl. Numer. Methds. Eng. **39** (1996), 2725–2741.
- [26] Y. Krongauz and T. Belytschko, *Consistent pseudo-derivative in meshless methods*, Comput. Meth. Appl. Mech. Eng. **146** (1997a), 371–386.
- [27] P. Lancaster and K. Salkauskas, *Surface generated by moving least squares methods*, Mathematics of Computation. **37** (1981), no. 155, 141–158.
- [28] W. K. Liu, S. Jun, and Y. Zhang, *Reproducing kernel particle methods.*, Int. Journl. Numer. Methds. Eng. **20** (1995), 1081–1106.
- [29] W. K. Liu, S. Li, and T. Belytschko, *Moving least square reproducing kernel methods part i: Methodology and convergence.*, Computer Methds. Appl. Mech. Eng. **143** (1997), no. 1-2, 113–154.
- [30] L. B. Lucy, *A numerical approach to the testing of the fission hypothesis.*, The Astronomical Journal. **82** (1977), no. 12, 1013–1024.
- [31] S. F. Mendez, J. Bonet, and A. Huerta, *Continuous blending of sph with finite elements.*, Computer and Structures. **83** (2005), no. 6, 1448–1458.
- [32] J. Monaghan, *An introduction to sph*, Comput. Phys. Commun. **48** (1988), 89–96.
- [33] B. Nayroles, G. Touzot, and P. Villon, *Generalizing the finite element method: diffuse approximation and diffuse elements.*, Comput. Mech. **10** (1992), 307–318.
- [34] E. Oñate and S. Idelsohn, *A mesh-free finite point method for advective-diffusive transport and fluid flow problems.*, Comput. Mech. **21** (1998), no. 4-5, 283–292.
- [35] E. Oñate, S. Idelsohn, O.C. Zienkiewicz, R. L. Taylor, and C. A. Sacco, *A stabilized finite point method of analysis of fluid mechanics problems.*, Computer Model. Eng. and Sci., **139** (1996), 315–346.
- [36] E. Oñate, F. Perazzo, and J. Miquel, *A finite point method for elasticity problems.*, Computer and Structures. **79** (2001), 2151–2163.
- [37] X. F. Pan, X. Zhang, and M. W. Lu, *Meshless galerkin least-squares method*, Computational Mechanics **35** (2005), 182–189.
- [38] S. H. Park and S. K. Youn, *The least squares meshfree method.*, Int. Journl. Numer. Methds. Eng. **52** (2001), 997–1012.
- [39] T. Rabczuk, T. Belytschko, and S. P. Xiao, *Stable particle methods based on lagrangian kernels*, Comput. Meth. Appl. Mech. Eng. **193** (2004), 1035–1063.
- [40] P. W. Randles and L. Libersky, *Smoothed particle hydrodynamics: some recent improvements and applications*, Comp. Methds. Appld. Mec. and Eng. **139** (1996), 375–408.
- [41] D. Shepard, *A two dimensional function for irregularly spaced data*, ACM National Conf. (1968).

- [42] H. Stolarski and T. Belytschko, *Membrane locking and reduced integration for curved elements*, J. Appl. Mech **49** (1982), 172–176.
- [43] J. W. Swegle, D. L. Hicks, and S. W. Attaway, *Smoothed particle hydrodynamics stability analysis*, J. Comput. Phys **116-1** (1995), no. 1, 123–134.
- [44] G. J. Warner and W. K. Liu, *Hierarchical enrichment for bridging scales and meshfree boundary conditions*, Int. J. Numer. Meths. Eng. **50** (2000), no. 3, 507–524.
- [45] Y. Wen, D. L. Hicks, and J. W. Swegle, *Stabilizing sph with conservative smoothing*, Tech. Report SAND94-1932-UC-705, Sandia National Laboratories, Albuquerque, NM, 1994.
- [46] S. P. Xiao and T. Belytschko, *Material stability analysis of particle methods*, Advanc. Computational Mathematics **23** (2005), 171–190.
- [47] X. Zhang, X. H. Liu, K. Z. Song, and M. W. Lu, *Least-squares collocation meshless method.*, Int. J. Numer. Meths. Eng.. **51** (2000), 1089–1100.
- [48] X. Zhang, K. Z. Song, M. W. Lu, and X. H. Liu, *Meshless methods based on collocation with radial basis functions.*, Comput. Mech. **51** (2000), 1089–1100.
- [49] T. Zhu and S. N. Atluri, *A modified collocation method and a penalty formulation for enforcing the essential boundary conditions in the element free galerkin method*, Comput. Mech. **21** (1998), no. 3, 211–222.